POLISH
JOURNAL *of* **RADIOLOGY**

Original paper

Congenital lung malformations: can we avoid computed tomography? A five-year study

Filomena Carfagnini[1,A,B,C,D,E,F], Donatella Vivacqua[1,A,B,C,D,E,F], Michelangelo Baldazzi[1,A,B,C,D,E,F], Laura Marcolin[1,A,B,C,D,E,F], Stefano Giusto Picchi[2,A,B,C,D,E,F], Giulia Lassandro[2,A,B,C,D,E,F], Igino Simonetti[3,B,C,D,E,F], Piero Trovato[4,A,B,C,D,E,F], Giuliana Giacobbe[5,A,B,C,D,E,F], Antonio Corvino[6,A,B,C,D,E,F], Laura Greco[1,A,B,C,D,E,F]

[1]Radiology Unit, Department of Experimental, Diagnostic and Speciality Medicine, Sant'Orsola Hospital, University of Bologna, Bologna, Italy
[2]General and Interventional Radiology, Diagnostic Imaging Department, Oncological Radiotherapy and Haematology, Diagnostic Imaging Area, Fondazione Policlinico Universitario A. Gemelli IRCCS, Rome, Italy
[3]Radiology Division, "Istituto Nazionale Tumori – IRCCS – Fondazione G. Pascale, Napoli, Italia", Naples, Italy
[4]Radiology Unit, "Santa Maria delle Grazie" Hospital, Pozzuoli, Italy
[5]Department of Precision Medicine, University of Campania "L. Vanvitelli", Naples, Italy
[6]Movement Sciences and Wellbeing Department, University of Naples "Parthenope", Naples, Italy

Abstract

Purpose: Congenital lung malformations (CLMs) consist of a variety of pulmonary development disorders. In the CLM approach, computed tomography (CT) is considered the gold standard imaging technique due to the high-resolution for the lung parenchyma evaluation, the study of the vascular system after contrast injection, and the multiplanar reconstructions. In the paediatric population CT is considered too invasive due to ionizing radiation and the use of contrast agent. Therefore, the indications for the use of magnetic resonance imaging (MRI) are increasing. The aim of our study is to compare retrospectively MRI and CT in the evaluation of CLMs, to reduce or avoid the use of contrast-enhanced CT in the paediatric population.

Material and methods: We retrospectively evaluated 22 paediatric patients with prenatal diagnosis of CLMs. All the patients underwent postnatal MRI in the first 2 weeks of life (except for a patient) and pre-surgery contrast-enhanced CT. A total of 7 blinded radiologists divided into 3 different groups independently reviewed each MRI and CT examination. Sensitivity and specificity of radiologists with different years of experience on the field, as well as of MRI findings regarding every pathology, were evaluated using a ROC curve. The interobserver agreement regarding the MRI findings was also measured.

Results: Analysing the ROC curves, we observed that MRI provided a satisfactory accuracy for diagnosing most congenital pulmonary diseases.

Conclusions: Our study showed that MRI without contrast agent allows us to reach a CLM diagnosis in good agreement with contrast-enhanced CT, which is considered the gold standard imaging technique.

Key words: computed tomography, infant, magnetic resonance imaging, lung diseases, bronchopulmonary sequestration, contrast media.

Correspondence address:
Antonio Corvino, Movement Sciences and Wellbeing Department, University of Naples "Parthenope", via Medina 40, I-80133 Naples, Italy, e-mail: an.cor@hotmail.it

Introduction

Congenital lung malformations (CLMs) consist of a variety of pulmonary development disorders with a large spectrum of clinical and imaging features. CLMs can involve all respiratory system structures, such as lung parenchyma, trachea and bronchi, pulmonary or systemic arteries and veins, and they can be found as isolated malformations or combined ones.

Notably, they occur as a continuum of interrelated abnormalities [1] that can present as isolated or in association; some of them have exclusive or prevalent parenchymal involvement and normal arterial and venal vascularization, such as congenital lobar overinflation (CLO), bronchogenic cyst (BC), and congenital pulmonary airway malformation (CPAM). Other malformations show different degrees of vascular and pulmonary alterations (bronchopulmonary sequestration), and in some abnormalities, including arteriovenous malformation (AVM), there is an altered vascularity with a regular lung parenchyma [2]. In many cases, radiological features show a combination of multiple malformations, resulting in hybrid lesions [3].

All these malformations have an annual incidence of between 30 and 42 cases per 100,000 population [4,5]. Nowadays, a substantial proportion of congenital lung anomalies are detected prenatally, and only few of these lesions are discovered incidentally [6] at any age due to the onset of symptoms (e.g. infections) or during other diagnostic investigations.

In the CLM approach, computed tomography (CT) is considered the gold standard imaging technique due to the high-resolution CT for the lung parenchyma evaluation, the study of the vascular system after contrast injection, and the multiplanar reconstructions [6-8]. On the other hand, in the paediatric population CT is considered too invasive due to ionizing radiation and the use of contrast agent. Therefore, the indications for the use of magnetic resonance imaging (MRI) in paediatric respiratory system diseases are increasing.

To date, only a pilot study that compared MRI and CT in the postnatal evaluation of CLMs has been reported [7]. The aim of our study is to compare retrospectively MRI and CT in the diagnosis and evaluation of CLMs, to reduce or avoid the use of contrast-enhanced CT in the paediatric population.

Material and methods

Patients

We retrospectively evaluated 22 (14 males and 8 females) patients with prenatal (foetal US) diagnosis of CLM. All the patients had been hospitalized at birth in our centre between January 2015 and December 2019 and had undergone postnatal MRI in the first 2 weeks of life (except for a patient who underwent MRI at the age of 18 days) and pre-surgery contrast-enhanced CT, usually at 3-6 months of life, for the study of CLMs. No patient underwent an MRI and a CT scan on the same day. For both MRI and CT, the scanned area extended from the pulmonary apex to the plane of the renal hila. Both techniques were performed in spontaneous breathing and in deep sedation.

MRI protocol

All patients underwent a 1.5-T MRI (Ingenia 1.5 T, Philips) study without contrast injection, in a supine position, with a mean scan time of about 20 minutes. MRI images were obtained with the following sequences: respiratory-triggered, T2-weighted turbo spin echo (TSE MultiVane) in axial, coronal, and sagittal planes (TR 1900 ms, TE 100 ms, Voxel 1.1 × 1.1 × 3 mm), and cardiac-triggered with respiratory gating 3D turbo field echo (FFE) T1 Dixon in the coronal plane with a reconstruction in the axial and coronal planes (TR 5.8 ms, TE 1.74 ms, flip angle 15°, Voxel 1.3 × 1.5 × 1.5 mm).

CT protocol

All CT studies were performed with a 64-slice CT scanner (GE Light Speed VCT) and a single-acquisition post-contrast protocol. All CT studies were performed with 80 kV and 3 mAs. The computed tomography dose index (CTDI vol) range was 0.8-1.4 mGy, and the dose-length product (DLP) range was 10-16 mGy × cm. The CT images were acquired with 2.5 mm slice thickness and reconstructed with 1.25 mm slice thickness in the axial, coronal, and sagittal planes with a pulmonary and mediastinal window. Maximum and minimum intensity projections (MIP and MinIp) were also performed. All patients received a non-ionic contrast (Iomeron 350 100 ML FL) at the dose of 2 ml/kg and injection rate of 0.8-1 ml/s, followed by a saline chaser at the dose of 3 ml/kg, also in relation to the condition of the patient, at the same injection rate.

Images analysis

A total of 7 radiologists divided into 3 different groups (2 groups of radiologists with 10 and 5 years of experience in paediatric radiology, respectively, and one group of radiology residents) independently reviewed the MRI and CT exams of each patient on a PACS workstation (CARESTREAM). The radiologists were blinded to the identity and the anamnestic data of all the patients and to any prenatal and postnatal exams. All paediatric radiologists first reviewed MRI images while the corresponding CT images were reviewed in a different session after 3 weeks. The exams were displayed in casual order in both sessions. The agreement between MRI and CT was assessed eva-

luating the malformation localization (side, lobe) and the presence or absence of the following elements, specific for the different and most common congenital pulmonary malformation (CLO, BC, CPAM, bronchial atresia, and bronchopulmonary sequestration): (i) cysts, (ii) overinflation and/or bronchocele, (iii) solid component, and (iv) presence and origin of abnormal arteries and/or venous drainage.

Congenital lobar overinflation results from a primary cartilage deficiency or dysplasia of a lobar bronchus, most commonly the left upper lobe. It is a condition characterized by a hyper-inflated lobe with attenuated pulmonary vessels, and contralateral mediastinum shift.

Bronchogenic cysts are thought to be due to abnormal budding during lung development. If they occur early in lung development, the cyst will be mediastinal, often carinal, and those that occur later in development will be intraparenchymal. They are well-defined hypoattenuating lesions with uniform fluid attenuation on CT and always demonstrate high signal intensity on T2-weighted MRI images (Figure 1).

CPAMs are described as hamartomatous tissue, with communication to the airway, normal arterial supply, and venous drainage and are subdivided according to the Stocker classification [7] into type 1 (cysts greater than 2 cm with presumed bronchial/bronchiolar origin), type 2 (cysts less than 2 cm with presumed bronchiolar origin); and type 3 (appears solid or shows very small cysts [< 0.2 cm] with presumed bronchiolar/alveolar origin) (Figure 2).

Bronchial atresia is characterized by atresia or stenosis of a lobar, segmental, or subsegmental bronchus at or near its origin. This results in a blind-ended atretic proximal bronchus, the distal portion of which dilates with a variable amount of mucus (bronchocele) and overinflation of the distal lung (Figure 3).

Bronchopulmonary sequestrations are a congenital mass of pulmonary tissue that has no normal connection with the tracheobronchial tree and is supplied by an anomalous systemic artery, usually arising from the descending aorta or abdominal aorta. There are 2 types of sequestration: intra-lobar sequestration is contained within the visceral pleura, and the venous drainage is usually via the pulmonary veins into the left atrium; extra-lobal sequestration has its own separate pleural investment, and the venous drainage is usually to the inferior vena cava or the azygous system (Figure 4) [9,10].

The reference standard used was the histologic report of each patient. This retrospective study was done in accordance with the Declaration of Helsinki. All patients' parents provided written informed consent.
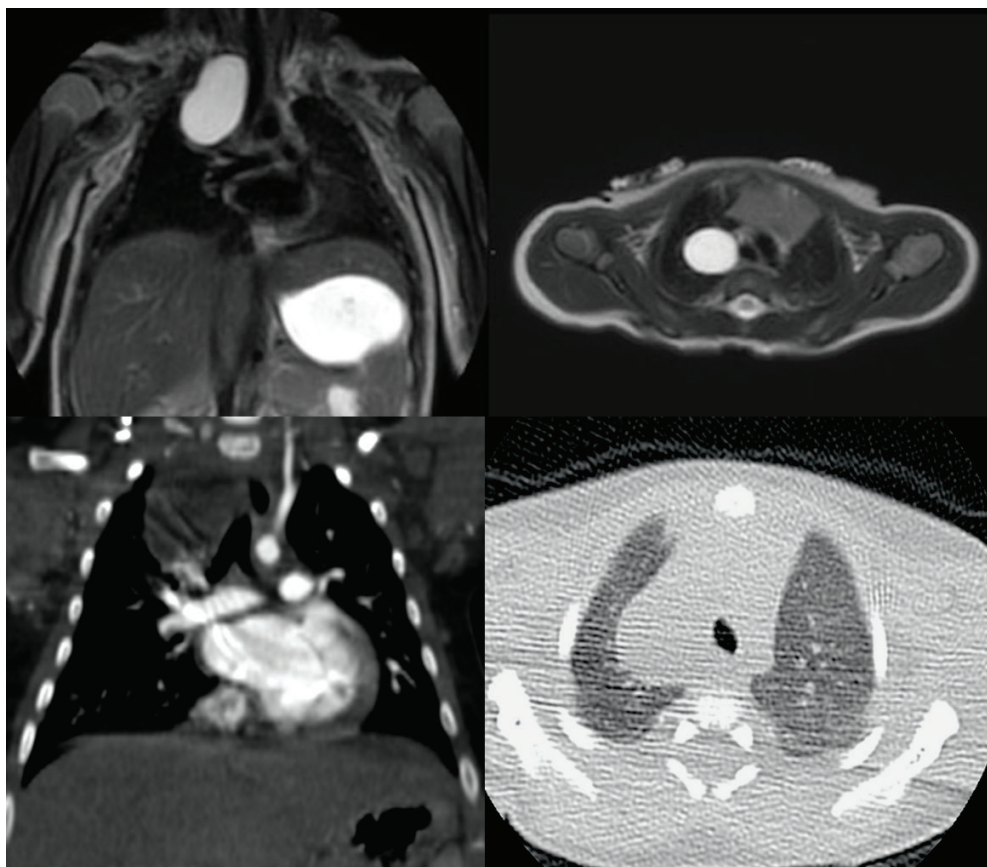

Figure 1. T2-weighted magnetic resonance imaging (MRI) (up) and contrast-enhanced computed tomography (CT) (down) on coronal and axial planes, showing a right paratracheal bronchogenic cyst. Bronchogenic cysts are well-defined fluid-filled lesions that always demonstrate high signal intensity on T2-weighted MRI images and fluid density on CT scans. Furthermore, we can note no enhancement of the lesion in the coronal CT scan
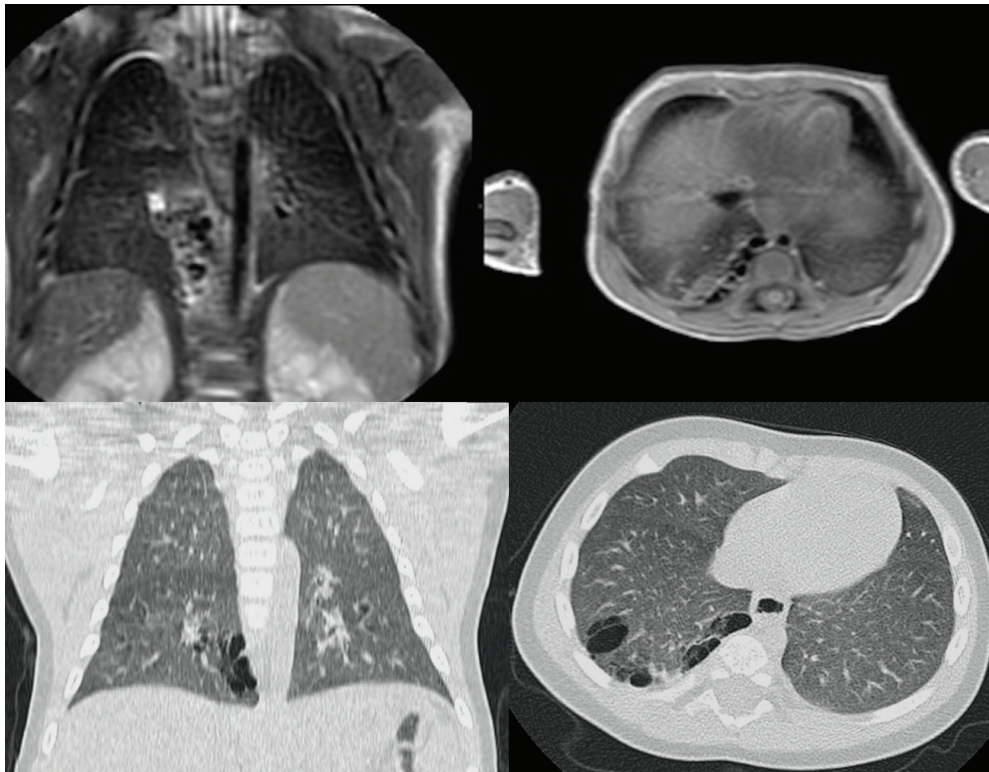
Figure 2. T2-weighted magnetic resonance imaging (MRI) (up) and lung window computed tomography (CT) (down) on coronal and axial planes, revealing hamartomatous tissue in the lower right lung. This finding is featured by multiple cysts smaller than 2 cm (type 2 congenital pulmonary airway malformation). As we can see in the coronal plane MRI scan, one of the cysts is fluid filled, and it demonstrates hyperintensity on T2-weighted MRI images
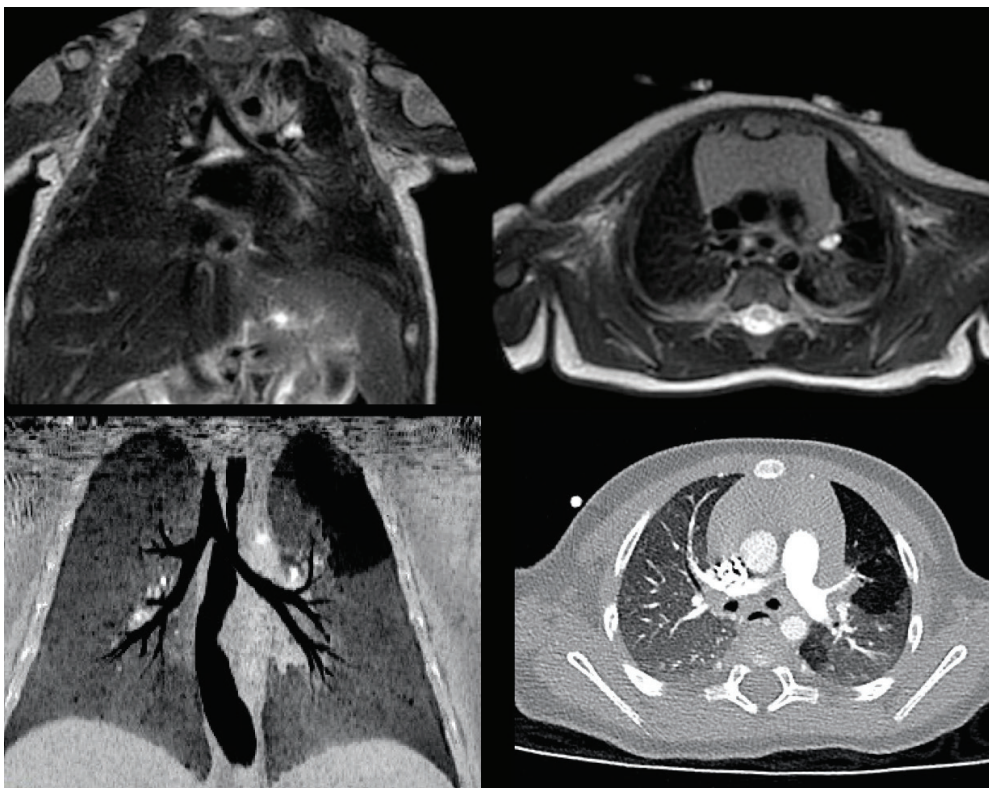

Figure 3. T2-weighted magnetic resonance imaging (up) and lung window computed tomography (CT) (down) on coronal and axial planes, whit minimum intensity projection (MinIP) reconstruction in the CT coronal plane, showing atresia of the origin of the left apicoposterior bronchus (B1 + 2). The bronchial atresia resulted in a bronchocele, a blind-ended atretic bronchus filled by mucus, and in the subsequent overinflation of the parenchyma involved
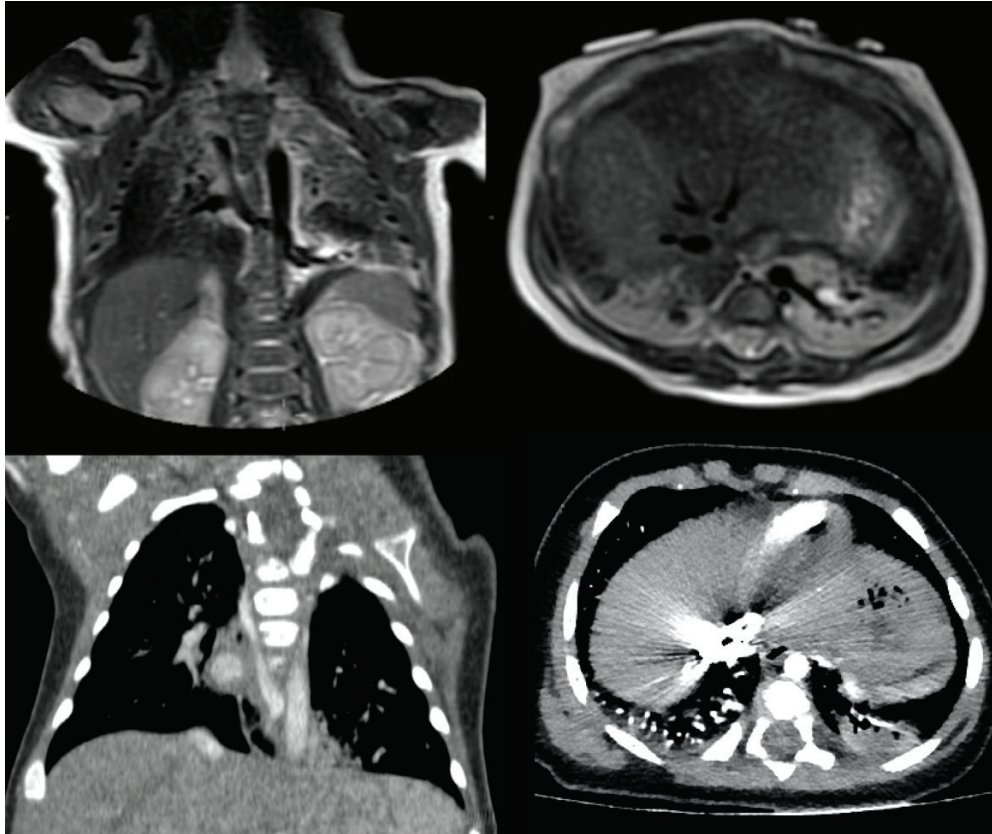
Figure 4. T2-weighted magnetic resonance imaging (up) and contrast-enhanced computed tomography (down) on coronal and axial planes, showing lower left lung extra-lobar bronchopulmonary sequestration. In the coronal plane (left) the venous drainage into the azygous system can be seen. In the axial plane (right) the anomalous artery supply arising from the descending aorta can be seen

Statistical analysis

Sensitivity and specificity of radiologists with different years of experience in the field, as well as of MRI findings regarding every pathology, were evaluated using a ROC curve. The interobserver agreement regarding the MRI findings was measured between interns and radiologists with > 10 years of experience using the κ statistic. P-values < 0.05 were considered significant. Data were analysed using IBM SPSS 22.0.0.

Results

A total of 22 patients (14 M and 8 F) were analysed; the age of the population at the time of the enrolment ranged between 1 and 18 days. At the histological analysis, taken as the reference standard diagnosis, we reported 6 CPAMs (4 CPAMs II and 2 CPAMs III), 6 bronchopulmonary sequestrations, 5 bronchial atresias, and 5 hybrid lesions (one bronchial atresia + CPAM and 4 bronchopulmonary sequestrations + CPAMs). One patient had a bilateral lesion, and 2 patients had a lesion extended under the diaphragm. 57% of the malformations were in the left hemithorax, and only 3 malformations involved the superior lobes (86% of the malformations were located in the lower lobes). The agreement on the localization (side and lobe) of the different malformations between MRI, CT, and histological reports was excellent. CT correctly identified 95% of all findings.

MRI findings ROC curves

We analysed the AUC of the ROC curves, computed for interns, radiologists with < 5 years of experience, and radiologists with > 10 years of experience. The results are reported in Table 1. We observed that MRI provided satisfactory accuracy for diagnosing most congenital pulmonary diseases. The presence of cysts, solid component, bronchocele, and abnormal arteries are MRI findings that can be evaluated with good to optimal interobserver agreement, whereas abnormal venous drainage, specific for bronchopulmonary sequestration, is better evaluated by more experienced radiologists.

Interobserver agreement

The agreement regarding the MRI findings evaluated by residents and radiologists with >10 years of experience showed high values for every finding except for venous drainage (Table 2). The agreement regarding the MRI findings evaluated by residents and radiologists with > 10 years of experience showed high values for every finding.

Table 1. Evaluation of AUC, sensitivity, and specificity for different congenital lung malformations subdivided according to radiologists' experience in paediatric radiology

	AUC	95% CI	Sensitivity	Specificity	*p*-value
Radiologists with > 10 years of experience					
Bronchopulmonary sequestration	0.979	0.932-1.000	100%	95.8%	< 0.001
Atresia	0.985	0.951-1.000	100%	97.1%	< 0.001
CPAM	0.885	0.752-1.000	83.3%	93.7%	< 0.001
Radiologists with < 5 years of experience					
Bronchopulmonary sequestration	0.871	0.757-0.984	95.0%	79.2%	< 0.001
Atresia	1.000	1.000-1.000	100%	100%	< 0.001
CPAM	0.802	0.631-0.973	66.7%	93.7%	< 0.001
Residents					
Bronchopulmonary sequestration	0.883	0.794-0.972	93.3%	83.3%	< 0.001
Atresia	0.900	0.778-1.000	80.0%	100%	< 0.001
CPAM	0.865	0.752-0977	83.3%	89.6%	< 0.001
Total					
Bronchopulmonary sequestration	0.906	0.854-0.959	95.7%	85.5%	< 0.001
Atresia	0.952	0.895-1.000	91.2%	99.2%	< 0.001
CPAM	0.853	0.774-0931	78.6%	92.0%	< 0.001

CPAM – congenital pulmonary airway malformation

Table 2. Evaluation of the interobserver agreement rate for radiological signs (0.41-0.60 = moderate; 0.61-0.80 = substantial; 0.81-1.00 = perfect)

Factor	κ	*p*
Cysts	0.862	< 0.001
Solid component	0.722	< 0.001
Bronchocele	0.766	< 0.001
Abnormal arterial supply	0.953	< 0.001
Abnormal venous drainage	0.552	< 0.001
Hyperinflation	0.886	< 0.001

Discussion

CLMs consist of a continuum of pulmonary development abnormalities that can affect all structures of the respiratory system (lung parenchyma, trachea and bronchi, pulmonary or systemic arteries and veins) as isolated or combined abnormalities, resulting in a large variety of clinical and imaging features. CLMs are generally diagnosed prenatally with ultrasound (US), which is the primary imaging modality for foetal screening [3] due to its low invasiveness. It provides valuable information about the presence and size of a focal lung lesion [11], lung hypoplasia, mass effect, hydrops fetalis, and any other organ malformations, all of which affect the prognosis and management [12,13]. A foetal MRI carried out only in some cases, which may be helpful in more complicated cases and in lung volume quantification [14].

In our centre, newborns with prenatal suspect or diagnosis of CLM undergo MRI during the first 2 weeks of life to confirm the prenatal diagnosis and to make a preliminary surgical plan. In the first 3-6 months of life and just prior to surgical intervention, contrast-enhanced CT is performed to assess any evolution of the underlying pathology and to study any information not previously appreciable at MRI.

CT examinations are commonly performed in the paediatric population and offer many advantages, mainly a shorter execution time. Although CT examinations account for a relatively small percentage of imaging studies, they contribute a large percentage of the overall radiation dose from imaging [15,16]. CT invasiveness in children has been demonstrated in many studies. Brenner et al. estimated the lifetime cancer mortality risks attributable to the radiation exposure from a single CT in a one-year-old child to be 0.18% (abdominal) and 0.07% (head) [16]. Due to all these factors, in the paediatric population a risk-benefit analysis is performed for each CT exam. Notably, the number of CT examinations must be reduced whenever possible, performing them only when it is absolutely necessary and using a protocol that minimizes exposure, in accordance with ALARA (as low as reasonably achievable) principles [10,17,18]. Therefore, it is more often preferable to use MRI instead of CT in paediatric patients because of the absence of ionizing radiation and considering the increased safety profile of the MRI.

In our study we retrospectively evaluated 22 patients with histologically proven CLMs with post-natal MRI and

contrast-enhanced CT after 3-6 months. In all our cases, the histological report was taken as the diagnostic gold standard reference. We compared findings between MRI and contrast-enhanced CT, independently reviewed by 3 groups of radiologists with different experience in paediatric radiology (2 radiologists with more than 10 years of experience, 2 radiologists with less than 5 years of experience, and 3 radiology residents), evaluating concordances and differences between the 2 imaging techniques. In the past 5 years we have modified the MRI protocol study for CLMs to improve its diagnostic reliability in the recognition of a single sign of each disease, notably parenchymal signs (cysts, overinflation) and vascular abnormalities. Recently we established our latest MRI protocol using 2 sequences: respiratory-triggered, T2-weighted turbo spin echo (TSE MultiVane) and cardiac-triggered with respiratory gating 3D FFE T1 Dixon. The MultiVane sequences improve image contrast resolution by radial filling of the K space, which allows for high quality images that are less affected by motion artifacts. The radial filling of the K space over-samples its centre, which contains the maximum signal amplitude and contributes to the image contrast resolution, resulting in a high signal-to-noise ratio and high contrast. In the first MRI protocol we used balance fast field echo (FFE) sequences to create black-blood images for the vessels study without contrast agent, allowing diagnosis in cases of pulmonary sequestration [19]. Over time, we changed our MRI protocol by using cardiac-triggered 3D FFE T1 Dixon with respiratory gating, which allows a high spatial resolution (about 2 mm thickness) and is free of movement artifacts. Lastly, volumetric acquisition ensures reconstruction on all planes of space with a single T1 sequence, which adds information to the MultiVane TSE sequence.

Analysis of findings by comparing MRI, CT, and surgical reports showed complete agreement (100% of cases) on the location (side and lobe) of the CLM. It was also noted that 57% of the malformations were in the left hemithorax, and 86% of the malformations were in the lower lobes, while only 3 malformations affected the upper lobes. Analysing the AUC of the ROC curves, calculated for both residents and radiologists with < 5 years and > 10 years of experience, it was observed that MRI provided precise evaluations that allow the diagnosis in most CLMs. Moreover, the MRI evaluation showed a good inter-observer agreement among the 3 different groups in detecting the presence of cysts, solid component, bronchocele, and abnormal arteries, while the finding of abnormal venous drainage, specific for bronchopulmonary sequestration, allowed a better diagnosis, especially for radiologists with greater experience and therefore with greater diagnostic confidence in MRI (the group with > 10 years of experience).

Therefore, there was excellent agreement concerning MRI findings also among the residents and the radiologists with more than 10 years of experience, showing reliable and comparable values for each considered finding, except for the identification of venous drainage (Table 2). Our results clearly show the high diagnostic reliability of MRI for pulmonary sequestration. Identifying the venous efferent branch is the more difficult challenge in bronchopulmonary sequestration diagnosis; therefore, it was mainly recognized by the more experienced radiologists, who correctly distinguished intra-lobar forms from the extra-lobar ones in a higher percentage of cases than the other groups (Figure 5). On the other hand, the diagnosis of CLMs with prevalent or exclusive parenchymal aerial signs (such as cysts or overinflation) was slightly less accurate, in particular in the case of CPAM. In our opinion, this is related to the intrinsic evolutionary character of these diseases and to the higher probability that aerial signs evolve over time and appear more evident after weeks or months. This evolutionary character is mainly shown by air cysts with smaller diameter.
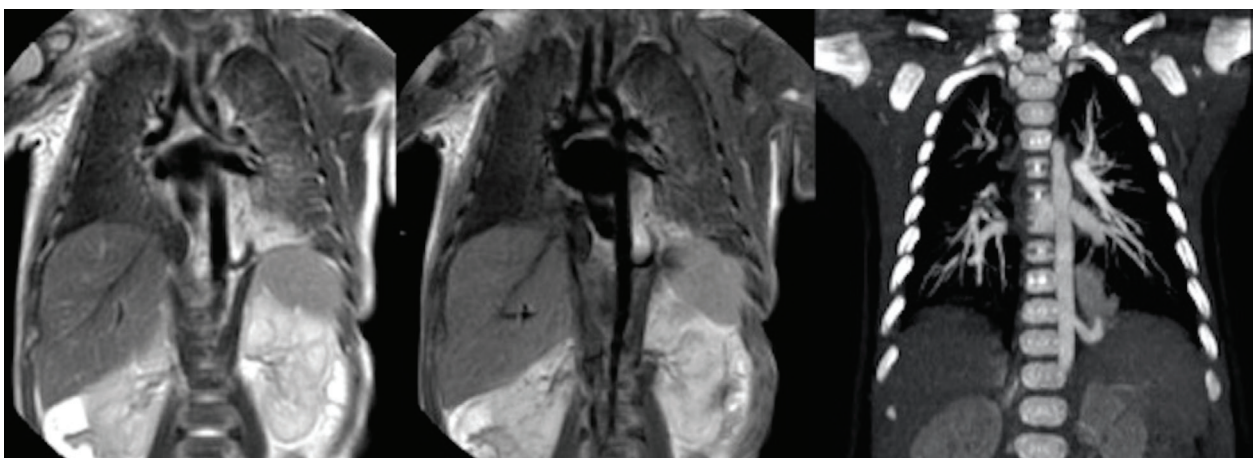

Figure 5. T2-weighted magnetic resonance imaging (MRI) (left), MRI minimum intensity projection (MinIP) reconstruction (central), and contrast-enhanced computed tomography (CT) maximum intensity projection (MIP) reconstruction (right) on coronal planes. Good concordance among contrast-enhanced CT and MRI MinIP reconstruction can be noticed, used for the better evaluation of the abnormal artery supply and venous drainage, in the diagnosis of bronchopulmonary sequestration in the lower left lung
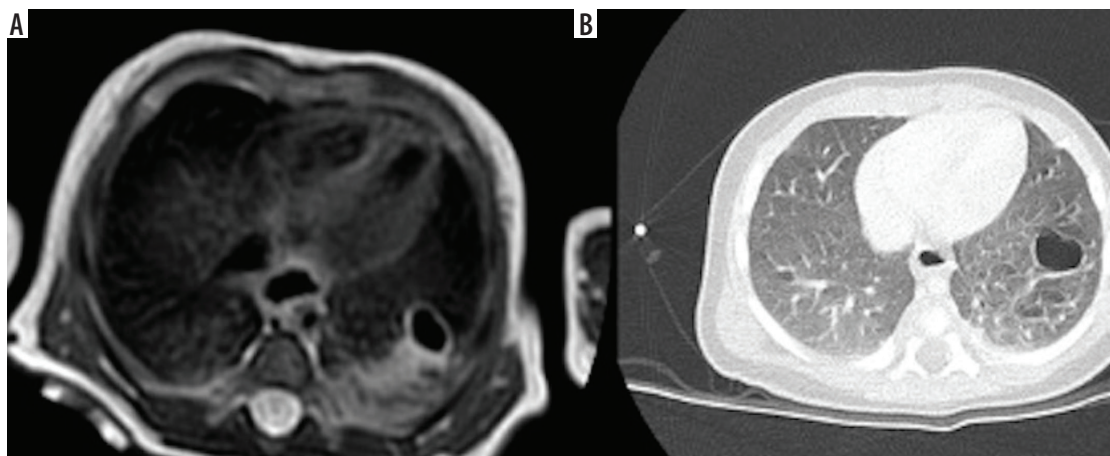
Figure 6. Magnetic resonance imaging acquired 7 days after birth (**A**) showing hamartomatous tissue and a unique cyst greater than 2 cm, pattern diagnosed as type 1 congenital pulmonary airway malformation (CPAM). Computed tomography (CT) acquired in the same female infant 6 months after birth (**B**), confirming type 1 CPAM diagnosis. As can be seen in the CT scan image (**B**), the cyst has a greater diameter because of the evolution of the disease over time
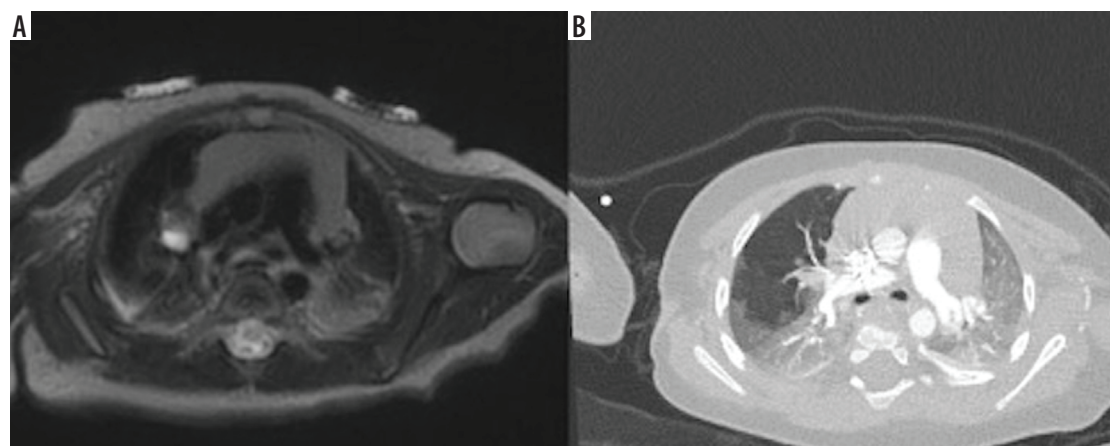

Figure 7. T2-weighted magnetic resonance imaging on axial planes (**A**) and contrast-enhanced computed tomography (CT) (**B**) showing right bronchial atresia with bronchocele. CT was acquired in the same infant about 6 months after birth, revealing the intrinsic evolutionary character of this congenital lung malformation: the overinflation is more evident in the CT images due to the more dedicated technique for the pulmonary parenchyma study both because the disease has evolved over time

Therefore, by performing MRI shortly after birth and a CT scan at 3-6 months of life, the CLMs have often evolved, creating a discrepancy in MRI and CT findings. This discrepancy may be only due to the pathological evolution of the diseases and not to the increased accuracy of CT in the lung parenchyma evaluation (Figures 6 and 7). It should also be remembered that these aerial signs often occur in the context of hybrid malformations, especially those in which lung sequestration coexists. In such cases the radiological finding of lung sequestration (a solid mass with systemic arterial afference, systemic venous or pulmonary drainage) initially dominates the MRI objectivity.

Our study still has some limitations: it is a monocentric study with a small sample, and MRI was voluntarily performed without contrast agent due to the patients age, reducing the potential of the technique. This problem was partly solved by improving the MRI protocol with the use of more performing sequences (TSE MultiVane and cardiac triggered with respiratory gating 3D FFE T1

Dixon). The main advantage is certainly the non-use of ionizing radiation with MRI and the high contrast resolution through dedicated protocols usage, which allowed us to reach the diagnosis even among radiologists with different experience.

Conclusions

Our study showed that MRI without contrast agent allows the CLM diagnosis to be reached in good agreement with contrast-enhanced CT, which is considered the gold standard imaging technique. We also believe that the small difference noted in our results between MRI and CT was mostly determined by the evolution of the disease, especially in the aerial components, because the 2 examinations were performed 3-6 months apart. Therefore, MRI without contrast agent and with dedicated and increasingly accurate protocols may represent a valid alternative in the postnatal diagnosis and management of CLMs, allowing an accurate diagnosis of these malformations.

Moreover, the diagnostic confidence acquired over years allowed us to better recognize the single sign of different disease, notably for the radiologists with longer experience in the specific field. We think that with larger studies non-contrast-enhanced MRI could become the first-line exam for diagnosis, follow-up, and preoperative planning of CLMs, avoiding useless ionizing radiation and contrast agent to the patient.

Conflict of interest

The authors report no conflict of interest.

References

1. Panicek DM, Heitzman ER, Randall PA, et al. The continuum of pulmonary developmental anomalies. Radiographics 1987; 7: 747-772.
2. Corvino F, Silvestre M, Cervo A, et al. Endovascular occlusion of pulmonary arteriovenous malformations with the ArtVentive Endoluminal Occlusion System™. Diagn Interv Radiol 2016; 22: 463-465.
3. Abbey P, Narula MK, Anand R. Congenital malformations and developmental anomalies of the lung. Curr Radiol Rep 2014; 2: 71. doi: https://doi.org/10.1007/s40134-014-0071-y.
4. Lee EY, Tracy DA, Mahmood SA, et al. Preoperative MDCT evaluation of congenital lung anomalies in children: comparison of axial, multiplanar, and 3D images. AJR Am J Roentgenol 2011; 196: 1040-1046.
5. Wall J, Coates A. Prenatal imaging and postnatal presentation, diagnosis and management of congenital lung malformations. Curr Opin Pediatr 2014; 26: 315-319.
6. Thacker PG, Rao AG, Hill JG, Lee EY. Congenital lung anomalies in children and adults. Current concepts and imaging findings. Radiol Clin North Am 2014; 52: 155-181.
7. Zirpoli S, Munari AM, Primolevo A, et al. Agreement between magnetic resonance imaging and computed tomography in the postnatal evaluation of congenital lung malformations: a pilot study. Eur Radiol 2019; 29: 4544-4554.
8. Stocker JT, Madewell JE, Drake RM.Congenital cystic adenomatoid malformation od the lung. Classification and morphologic spectrum. Hum Pathol 1977; 8: 155-171.
9. Lee EY, Dorkin H, Vargas SO. Congenital pulmonary malformations in pediatric patients: review and update on etiology, classification, and imaging findings. Radiol Clin North Am 2011; 49: 921-948.
10. Epelman M, Kreiger PA, Servaes SV, et al. Current imaging of prenatally diagnosed congenital lung lesions. Semin Ultrasound CT MR 2010; 31: 141-157.
11. Crombleholme TM, Coleman B, Hedrick H, et al. Cystic adenomatoid malformation volume ratio predicts outcome in prenatally diagnosed cystic adenomatoid malformation of the lung. J Pediatr Surg 2002; 37: 331-338.
12. Usui N, Kamata S, Sawai T, et al. Outcome predictors for infants with cystic lung disease. J Pediatr Surg 2004; 39: 603-606.
13. Khalek N, Johnson MP. Management of prenatally diagnosed lung lesions. Semin Pediatr Surg 2013; 22: 24-29.
14. Recio Rodríguez M, Martínez de Vega V, Cano Alonso R, et al. MR imaging of thoracic abnormalities in the fetus. Radiographics 2012; 32: E305-321. doi: 10.1148/rg.327125053.
15. Kim JE, Newman B. Evaluation of a radiation dose reduction strategy for pediatric chest CT. AJR Am J Roentgenol 2010; 194: 1188-1193.
16. Mettler FA Jr, Wiest PW, Locken JA, et al. CT scanning: patterns of use and dose. J Radiol Prot 2000; 20: 353-359.
17. Brenner D, Elliston C, Hall E, et al. Estimated risks of radiation-induced fatal cancer from pediatric CT. AJR Am J Roentgenol 2001; 176: 289-296.
18. Greenwood TJ, Lopez-Costa RI, Rhoades PD, et al. CT dose optimization in pediatric radiology: a multiyear effort to preserve the benefits of imaging while reducing the risks. Radiographics 2015; 35: 1539-1554.
19. Fuchs F, Laub G, Othomo K. TrueFISP – technical considerations and cardiovascular applications. Eur J Radiol 2003; 46: 28-32.